

Determination of DNA minor groove width in distamycin-DNA complexes by solid-state NMR

Greg L. Olsen, Elizabeth A. Louie, Gary P. Drobny and Snorri Th. Sigurdsson*

Department of Chemistry, University of Washington, Seattle, WA 98195-1700, USA

Received May 12, 2003; Revised and Accepted July 16, 2003

ABSTRACT

We have performed solid-state ^{31}P - ^{19}F REDOR nuclear magnetic resonance (NMR) experiments to monitor changes in minor groove width of the oligonucleotide d(CGCAA $^{2\text{F}}$ UTGGC)-d(GCCAAT(pS)TTGCG) (A_3T_2) upon binding of the drug distamycin A at different stoichiometries. In the hydrated solid-state sample, the minor groove width for the unbound DNA, measured as the $^{2\text{F}}\text{U7}$ -pS19 inter-label distance, was 9.4 ± 0.7 Å, comparable to that found for similar A:T-rich DNAs. Binding of a single drug molecule is observed to cause a 2.4 Å decrease in groove width. Subsequent addition of a second drug molecule results in a larger conformational change, expanding this minor groove width to 13.6 Å, consistent with the results of a previous solution NMR study of the 2:1 complex. These ^{31}P - ^{19}F REDOR results demonstrate the ability of solid-state NMR to measure distances of 7–14 Å in DNA–drug complexes and provide the first example of a direct spectroscopic measurement of minor groove width in nucleic acids.

INTRODUCTION

The interactions of proteins and small molecules with nucleic acids have long been a subject of extensive study. In light of the biological importance of nucleic acid complexes, a wide array of biochemical, biophysical and spectroscopic techniques have been used to pursue an atomic level understanding of recognition, binding specificity and structural alterations associated with complex formation. Solid-state NMR can provide important structural and dynamic information about biomolecules and biomolecular complexes, including many systems which are not tractable to X-ray crystallographic or solution NMR analysis (1–6). In particular, when the distances to be measured exceed those observable via solution NMR or when suitable crystals cannot be obtained for X-ray studies, solid-state NMR experiments in conjunction with site-specific isotopic labeling can often allow access to otherwise difficult to obtain inter-atomic distance information. During the past decade, the rotational echo double resonance (REDOR) experiment (7,8) has emerged as the primary solid-state NMR technique for determination of selected heteronuclear

dipolar coupling values and has thus become a valuable method for internuclear distance measurement in structural studies of biological systems (reviewed in 8–10).

A particularly important type of DNA–ligand interaction is that of small molecules with the minor groove. Distamycin A is a short naturally occurring peptide antibiotic (Fig. 1), which has been shown to bind non-covalently in the minor groove of A:T-rich B-DNA tracts (11). As distamycin–DNA complexes have been extensively characterized (11–20), they provide useful model systems for solid-state NMR structural studies of nucleic acid complexes. We have performed REDOR experiments to monitor changes in minor groove width in the oligonucleotide d(CGCAA $^{2\text{F}}$ UTGGC)-d(GCCAAT(pS)-TTGCG) (A_3T_2) upon binding of the drug distamycin at 0:1, 1:1 and 2:1 drug:DNA ratios. Binding of distamycin to A_3T_2 occurs either in the form of a 1:1 complex or as a 2:1 complex: the minor groove can accommodate not only a single distamycin molecule, but also side-by-side antiparallel binding of two distamycin molecules (15,16). It may thus be inferred that distamycin binding at the different ratios must be accompanied by significant deformations of the A_3T_2 minor groove. The present REDOR measurements confirm this, showing a 2 Å decrease in minor groove width upon 1:1 binding and a subsequent 6 Å increase upon formation of the 2:1 complex. These experiments are, to our knowledge, the first example of the use of a spectroscopic technique for direct measurement of groove width in DNA.

MATERIALS AND METHODS

Sample preparation

DNA oligomers d(CGCAA $^{2\text{F}}$ UTGGC) and d(GCCAAT-(pS)TTGCG) were synthesized on an ABI 394 DNA/RNA synthesizer, deprotected in NH_4OH at 55°C for 16 h, then HPLC purified on a C18 column. Following detritylation (4:1 $\text{AcOH}/\text{H}_2\text{O}$ v/v, 40 min, room temperature) and evaporation of the solvent, the oligonucleotides were ethanol precipitated, desalted using Sep-Paks or RP-HPLC, filtered (0.40 μm Alltech nylon) and characterized using analytical denaturing PAGE and electrospray mass spectroscopy. Alternatively, the oligonucleotides were gel purified following detritylation. The purified oligos were dissolved in water and salted by addition of 0.01 M Na_2EDTA and 1.71 M NaCl (final composition 10% Na_2EDTA and 10% NaCl by weight upon lyophilization). Annealing of the DNAs was accomplished by heating this solution to 80°C for 7 min, then cooling to room temperature.

*To whom correspondence should be addressed. Tel: +1 206 616 8276; Fax: +1 206 685 8665; Email: sigurdsson@chem.washington.edu

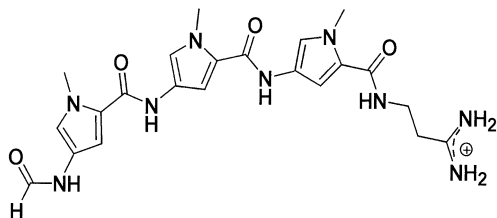


Figure 1. Chemical structure of the minor groove binder distamycin.

The sample was lyophilized and duplex formation verified by non-denaturing PAGE.

The unbound (0:1) DNA sample was run as a frozen solution. A 5.11 μmol aliquot of the lyophilized, salted duplex DNA was dissolved in 50 μl of H_2O , then placed in the MAS rotor.

Distamycin A hydrochloride (Sigma) was used without further purification. The 1:1 drug:DNA sample was prepared by dissolving 1.833 μmol of the salted unbound DNA in H_2O (1.0 ml), adding 514 μl (1.835 μmol) of a freshly prepared 3.57 mM solution of distamycin HCl dissolved in 50 mM sodium cacodylate (pH 6.0), then equilibrating overnight at room temperature. The sample was frozen using liquid nitrogen, lyophilized, returned to the MAS rotor and hydrated by vapor diffusion to 23 waters per nucleotide ($W = 23$). W values were determined gravimetrically following equilibration in a sealed 85% relative humidity chamber. To verify that sample loss or evaporation were not occurring, sample weight was monitored throughout the course of the experiments. The 2:1 complex was formed by redissolving the 1:1 sample in H_2O (0.5 ml), adding 514 μl of a freshly prepared 3.57 mM solution of distamycin HCl dissolved in H_2O (1.835 μmol), then shaking gently overnight at room temperature. The sample was frozen using liquid nitrogen, lyophilized, returned to the MAS rotor and hydrated to $W = 13$.

As three different species, the unbound DNA, DNA in 1:1 complexes and DNA in 2:1 complexes, are expected to be present in the 1:1 sample, simulation of REDOR dephasing for this sample requires determination of their relative populations. If the 9:1 ratio of 1:1 to 2:1 complexes observed in a 0.75:1 drug:DNA mixture (15) is assumed to persist after addition of the additional 0.25 equivalents of drug needed to reach the 1:1 stoichiometry, the relative populations may be estimated as follows: (fraction of DNA in 1:1 complexes) + $2 \times$ (fraction of DNA in 2:1 complexes) = total distamycin equivalents = 1.0, and (fraction 1:1)/(fraction 2:1) = 9/1. Thus (fraction 1:1) = $9 \times$ (fraction 2:1), and $1.0 = 9 \times$ (fraction 2:1) + $2 \times$ (fraction 2:1) = $11 \times$ (fraction 2:1) or (fraction 2:1) = $1.0/11 = 0.0909 \approx 9\%$, leaving (fraction 1:1) = $9 \times$ (fraction 2:1) = $0.8181 \approx 82\%$, with the remaining 9% of the DNA unbound.

NMR spectroscopy

All experiments were performed in a home built spectrometer with a 4.7 T field (200 MHz proton Larmor frequency), using a home built triply tuned HFP MAS probe (21). All measurements were made at -30°C , with magic angle spinning at 5988 ± 2 Hz. Sample cooling used controlled temperature dry air, generated using an FTS Systems TC-84 controller and

XR11851A cooling unit and applied directly to the MAS rotor. rf field strengths were regulated to within $\pm 1\%$, spinning speed to within ± 2 Hz and sample temperatures to within $\pm 1^\circ\text{C}$. All REDOR experiments employed XY-8 phase cycling on both the ^{31}P and the ^{19}F channels. Custom made 4 mm zirconia rotor barrels were purchased from O'Keeffe Ceramics. Rotor tips and end caps were prepared in-house.

Unbound DNA (0:1) sample. Proton pulse- and cross-polarization rf fields were 50 kHz ($5.0 \mu\text{s } T_{90}$), with 102 kHz proton decoupling. Phosphorus and fluorine rf pulse fields were 50 and 71 kHz (10.0 and $7.0 \mu\text{s } T_{180\text{S}}$, respectively). CP contact time was 1.2 ms. 1024 points were acquired, with a dwell time of 25 μs . Nine REDOR S and S_0 data point pairs were acquired, at 1.33 ms (8 rotor period, 1 REDOR cycle) intervals. Acquisition time was 25.6 ms and recycle delay was 2 s. 6174 scans were recorded for each REDOR S or S_0 data point. Four data sets were collected (63 h each) and summed.

(1:1) sample. Proton pulse- and cross-polarization rf fields were 55 kHz ($4.5 \mu\text{s } T_{90}$), with 114 kHz proton decoupling. Phosphorus and fluorine rf pulse fields were 50 and 67 kHz (10.2 and $7.4 \mu\text{s } T_{180}$, respectively). CP contact time was 2.0 ms. 1024 points were acquired, with a dwell time of 25 μs . Acquisition time was 25.6 ms and recycle delay was 2 s. Six REDOR S and S_0 data point pairs were acquired, at 1.33 ms (8 rotor period, one REDOR cycle) intervals. (Due to rapid dephasing, this experiment was adjusted to collect S and S_0 points at the shorter intervals.) 4096 scans were recorded for each REDOR S or S_0 data point. Six data sets were collected (28 h each), then summed.

(2:1) sample. Proton pulse- and cross-polarization rf fields were 52 kHz ($4.8 \mu\text{s } T_{90}$), with 107 kHz proton decoupling. Phosphorus and fluorine rf pulse frequencies were 50 and 63 kHz (10.2 and $7.9 \mu\text{s } T_{180}$, respectively). CP contact time was 1.75 ms. 256 points were acquired, with a dwell time of 25 μs . Recycle delay was 3 s. Acquisition time was 6.4 ms. The shortened acquisition time for the 2:1 sample was used to allow application of a higher decoupling field while avoiding rf arcing.

An initial experiment showed minimal dephasing for the 2:1 sample, indicating that the P-F distance to be measured in this sample was significantly longer than for either of the two previous samples. To determine long ($>10 \text{ \AA}$) P-F distances, longer dephasing times are required. The associated reduction in signal to noise, however, necessitates significantly extended signal averaging times, and instrumental stability and time requirements then prohibit acquisition of a full dephasing curve. In such cases, acquisition of a single REDOR point may be used to obtain the internuclear separation (3). Hence, to enable measurement of the longer distance, a single dephasing time, 14.7 ms (11 REDOR cycles), was selected for application during a single shorter (6 day) signal averaging period. Data were acquired in 14 h (8192 scan) blocks, which were individually screened for arcing, then summed prior to processing.

Data processing

Data processing was performed using the Gullrington NMR processing suite (Gullrington: a computer program for

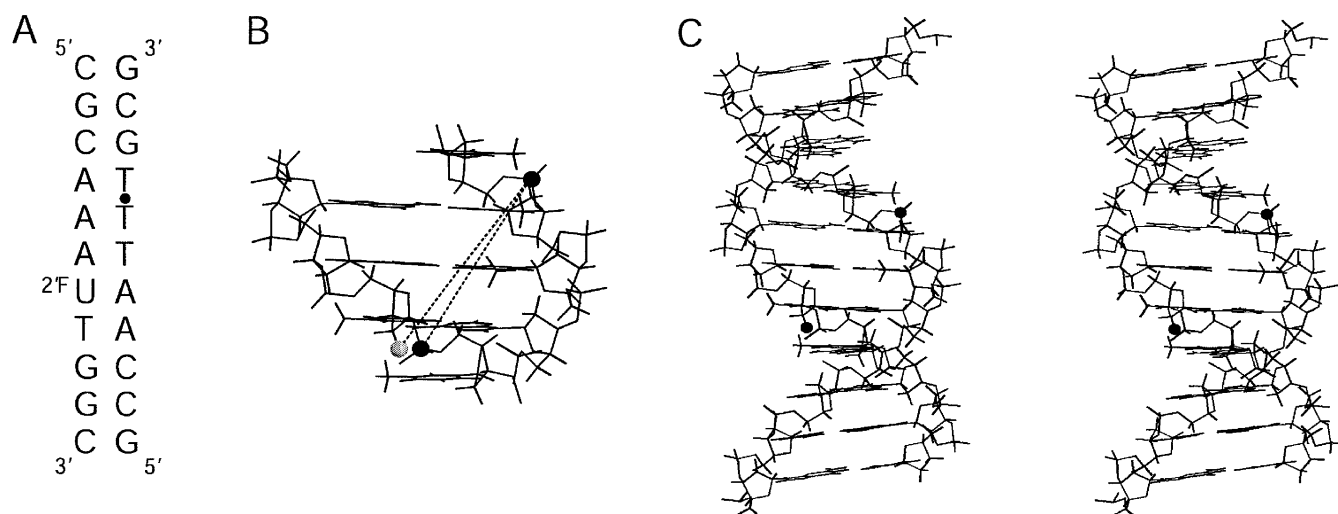


Figure 2. (A) The A_3T_2 DNA sequence used in this study. ^{2F}U indicates 2'-fluoro-2'-deoxyuridine and the dot between T18 and T19 denotes a phosphorothioate. (B) Expanded view of A_3T_2 DNA showing label positions corresponding to standard and P-F REDOR measures of minor groove width across the central A_3T_2 tract. The dark sphere at upper right marks the i phosphate (T19); on the lower left, the dark sphere indicates the $i + 3$ phosphate (T8), while the light sphere indicates the 2F label used in the present experiments. The standard B-form DNA model for the A_3T_2 oligomer was generated using the biopolymer module of Insight II (Biosym). (C) Stereoview of the free A_3T_2 DNA generated using Insight II. Dark spheres show location of phosphorothioate and ^{2F}U .

estimation of molecular properties from NMR experiments, T. Karlsson and G.P. Drobny, in preparation). All simulations were performed using Simpson (22). Reduced χ^2 plots were used to determine best fit distances and error bounds (90% confidence intervals).

RESULTS AND DISCUSSION

Measurement of DNA groove width

Direct measurement of minor groove width in DNA presents a spectroscopic challenge, as the distances to be measured exceed the range of NOE residual dipolar coupling measurements. For instance, upon widening of the minor groove to accommodate drug binding, the groove width will often exceed 10 Å (15,16,23–26). While such distances are currently beyond the reach of solution NMR methods, ^{31}P - ^{19}F REDOR has been used to determine internuclear distances of up to 16 Å, making it an ideal tool for the task (3,27). In the REDOR experiment, measurement of heteronuclear dipolar couplings is accomplished using 'dephasing' pulses during magic angle sample spinning to disrupt the averaging of the dipolar coupling. Application of these pulses to nuclei that are coupled to the observed spins produces an attenuated signal, which is then compared to a reference signal from a control experiment in which the dephasing pulses were omitted. Plotting the ratio of the experimental (S) and reference (S_0) signals versus evolution (dephasing) time, S/S_0 , allows extraction of the dipolar coupling constant, thus giving direct access to the internuclear distance. In particular, the observed decay in S/S_0 is dependent upon the number of rotor cycles (i.e. the dipolar evolution time) and on the dipolar coupling constant. Fitting of each observed REDOR dephasing curve to a simulation then allows determination of internuclear distances.

A common measure of minor groove width is the distance between a selected backbone phosphate i and the $i + 3$ phosphate on the opposing strand (28–32). To adapt this for observation of A_3T_2 via REDOR, the ^{31}P - ^{19}F distance was measured between phosphate T19 (i position) in the backbone and a 2'-fluoro-labeled uridine substituted at T7 directly across the groove (immediately 3' of the $i + 3$ phosphate) (Fig. 2). As can be seen in Figure 2, the two schemes represent quite similar measures of groove width. Since backbone phosphates have nearly the same chemical shift in solid-state NMR, replacement of the selected phosphate by a phosphorothioate was used to shift the corresponding phosphate resonance, resolving it from the large DNA phosphodiester backbone peak, thereby eliminating the need for phosphorus background correction (27). As the phosphoramidite of 2'-fluorouridine is commercially available, allowing easy insertion of a high sensitivity (high γ) heterospin for the REDOR measurements, and because incorporation of phosphorothioates is readily accomplished during DNA synthesis, this ^{31}P - ^{19}F labeling scheme allows rapid and inexpensive sample preparation, avoiding synthetic difficulties often associated with isotopic labeling in nucleic acids.

Distamycin is a minor groove binder

Double-helical DNA, in particular the B-form, is known to display sequence-dependent conformational variation (33,34). A:T-rich B-DNA tracts, for example, are observed to form an unusually narrow minor groove (13,28,33,35), which has been shown to be the preferred binding site for a number of small minor groove binding compounds (11). One of these, distamycin (Fig. 1), is a short peptide antibiotic containing three pyrrole rings and a positively charged propylammonium tail. Distamycin binds non-covalently in the minor groove of several A:T-rich sequences, using a combination of electrostatic, van der Waals and hydrogen bonding interactions

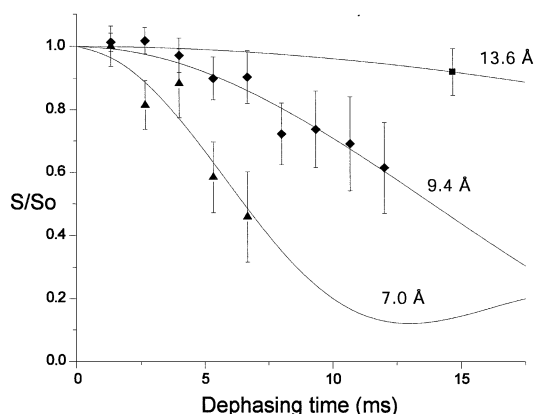


Figure 3. REDOR dephasing curves for A_3T_2 DNA and its 1:1 and 2:1 distamycin complexes. Solid lines represent expected decay curves based on simulations. Diamonds mark data for the unbound A_3T_2 DNA, triangles for the 1:1 distamycin: A_3T_2 complex and the square for the 2:1 distamycin: A_3T_2 complex. The lowest (7.0 Å) line represents a simulation for the 1:1 sample, where the fit is a weighted superposition of simulated dephasing curves corresponding to the three species present in the sample (unbound A_3T_2 and the 1:1 and 2:1 complexes), as described in the text.

(11,13–16,18,19,36). Solution NMR models place the distamycin amide protons in positions to hydrogen bond to acceptors on the floor of the minor groove and situate the drug pyrrole rings in close van der Waals contact to the walls of the groove (14–16). The cationic propylamidinium group of the drug contributes to electrostatic interactions between distamycin and the negative potential of the phosphate backbone (15,16). When bound, distamycin assumes an extended conformation, forming a crescent shape spanning 5 bp and conforming to the curvature of the minor groove. Solution NMR experiments on distamycin in complex with the 11mer used for the present experiments (Fig. 1) found that for this sequence, distamycin binds at the central A_3T_2 site as a monomer and side-by-side as an antiparallel dimer, to form both 1:1 and 2:1 complexes, respectively (15,16). Accordingly, to probe perturbations of the groove associated with formation of these complexes, we have measured the A_3T_2 minor groove width in samples at 0:1, 1:1 and 2:1 distamycin:DNA stoichiometries.

^{31}P - ^{19}F REDOR solid-state NMR measurements

Groove width in unbound DNA. The initial REDOR experiment, performed on A_3T_2 prior to addition of distamycin, was used to obtain the native groove width corresponding to our P-F label pair in the solid-state sample. The REDOR data for the unbound DNA are shown in Figure 3, where S/S_0 is plotted versus dephasing time. Comparison of the experimental results to simulated dephasing curves gives a χ^2 best fit groove width of 9.4 ± 0.7 Å. While neither X-ray crystal nor solution NMR structures are available for this DNA, structures for a collection of similar A:T-rich DNA sequences show corresponding (pS- ^{19}F) inter-label distances of 9.6–10.9 Å, which are in agreement with the present REDOR measurement (37–41).

Groove width in distamycin–DNA 1:1 complex. Following addition of one equivalent of the drug, the second REDOR

experiment was performed. Figure 3 shows the resulting dephasing curve obtained for the 1:1 sample. The observed rapid dephasing suggests a significant narrowing of the minor groove. One complicating factor in the determination of groove width from these data is the expected presence of several different species in the 1:1 sample. Solution NMR results for titration of distamycin with A_3T_2 indicate that three DNA species, the unbound DNA, the 1:1 complex and the 2:1 complex, should be present following addition of a single equivalent of the drug (15,16). A qualitative fit to the 1:1 sample data was obtained using the following two assumptions. First, the 9:1 ratio of 1:1 to 2:1 complexes observed in a 0.75:1 drug:DNA mixture (15) was assumed to persist after addition of the additional 0.25 equivalents of drug needed to reach the 1:1 stoichiometry. This assumption results in three approximate populations for the DNA within the 1:1 sample: ~82% bound in 1:1 drug:DNA complexes, ~9% in 2:1 complexes, with the remaining ~9% present as the unbound DNA (see Materials and Methods for calculation details). Second, the minor groove widths for the 0:1 and 2:1 samples were taken to be those measured in the present REDOR experiments, 9.4 and 13.6 Å, respectively. The REDOR dephasing curve is a superposition of curves corresponding to each of the three species present in the sample, weighted according to relative population. A single parameter, the minor groove width corresponding to the 1:1 complexes, was varied, with the remaining distances and populations fixed as described above. This fitting procedure yields a ^{31}P - ^{19}F distance of ~7.0 Å, a decrease of 2.4 Å relative to the corresponding distance in the unbound DNA.

Binding of one distamycin molecule thus appears to produce a significant narrowing of the DNA minor groove in the hydrated solid state. Decreases in minor groove width upon distamycin binding have previously been observed. For example, the analogous distance across the central AAT tract in the dodecamer d(CGCAAATTTGCG)₂ was found to decrease by ~0.7 Å in an X-ray structure of the 1:1 distamycin complex (13), relative to the unbound DNA (42).

Recent solution NMR studies and molecular dynamics simulations have shown a strong response of minor groove width to the local electrostatic environment, suggesting that electrostatic disturbances associated with distamycin occupancy of the minor groove could significantly affect the groove width (32,43–47). Hence, one possibility consistent with the present results is that upon distamycin binding, displacement of the minor groove spine of hydration or of counterions in the hydration shells provides such a perturbation of the electrostatic environment within the minor groove. Alternatively, enhancement of van der Waals contact between distamycin and the groove walls could be a driving force for a narrowed minor groove (11,13–16,31).

Groove width in distamycin–DNA 2:1 complex. Upon addition of a second equivalent of distamycin, solution NMR studies reveal that only those solution NMR cross-peaks corresponding to a 2:1 complex are present (15,16). The REDOR dephasing data for the 2:1 complex is shown in Figure 3, and Figure 4 shows the corresponding S and S_0 spectra. In contrast to the 1:1 complex, a significant increase in minor groove width, to 13.6 ± 1.5 Å, was observed for the 2:1 complex. The 2:1 groove width observed in the present experiment is in

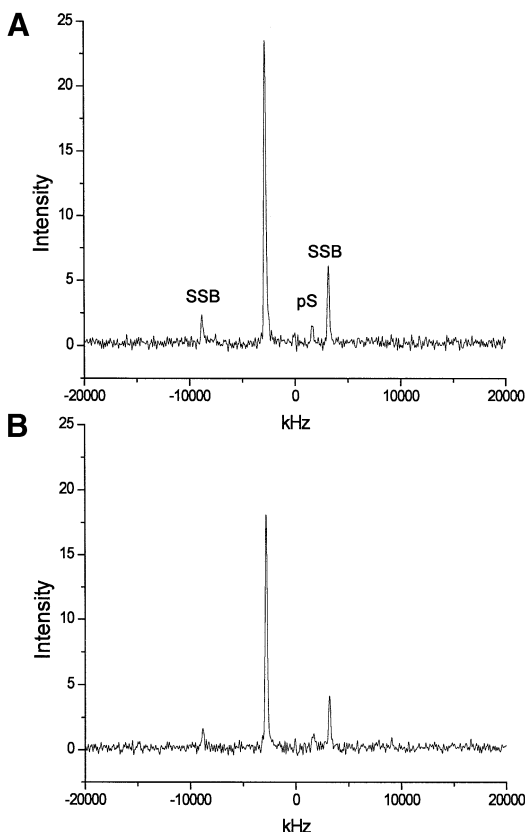


Figure 4. REDOR S and S_0 spectra for the 2:1 distamycin: A_3T_2 DNA complex. Plots were generated without line broadening and show absolute intensities. (A) Reference (S_0) ^{31}P spectrum, where pS denotes the phosphorothioate signal. The large central peak and its spinning side bands (SSB) are due to unmodified backbone phosphates. (B) Experimental (S) REDOR spectrum, showing diminished ^{31}P backbone and phosphorothioate peak intensities following application of ^{19}F pulses.

agreement with the distance seen in a model generated using solution NMR distance restraints (~ 13.1 Å; D. Wemmer, personal communication).

CONCLUSION

In summary, these results show large changes in DNA minor groove width as ligand stoichiometry is varied (Fig. 4). In the hydrated solid-state sample, binding of a single distamycin molecule to A_3T_2 generates a 2.4 Å decrease in groove width, while addition of a second drug molecule results in a large conformational change, expanding the minor groove width by 6.6 Å, to 13.6 Å. The 13 Å distance suggested by a previous solution NMR study for the 2:1 complex is supported by our data, demonstrating the ability of ^{31}P - ^{19}F REDOR to accurately measure distances of >10 Å in a nucleic acid complex. These solid-state NMR studies present, to our knowledge, the first example of direct spectroscopic measurement of minor groove width in nucleic acids.

ACKNOWLEDGEMENTS

We thank J. Markley for synthesis and purification of the DNA samples, D. Wemmer for use of the 2:1 distamycin-DNA

model coordinate file and the Drobny and Sigurdsson groups for critical review of the manuscript. This work was supported by a grant from the National Institutes of Health (GM58914).

REFERENCES

- Ketchum, R.R., Hu, W. and Cross, T.A. (1993) High-resolution conformation of gramicidin A in a lipid bilayer by solid-state NMR. *Science*, **261**, 1457–1460.
- Opella, S.J., Kim, Y. and McDonnell, P. (1994) Experimental nuclear magnetic resonance studies of membrane proteins. *Methods Enzymol.*, **239**, 536–560.
- Studelska, D.R., Klug, C.A., Beusen, D.D., McDowell, L.M. and Schaefer, J. (1996) Long-range distance measurements of protein binding sites by rotational-echo double resonance NMR. *J. Am. Chem. Soc.*, **118**, 5476–5477.
- Merritt, M.E., Christensen, A.M., Kramer, K., Hopkins, T. and Schaefer, J. (1996) Detection of intercatechol cross-links in insect cuticle by solid-state carbon-13 and nitrogen-15 NMR. *J. Am. Chem. Soc.*, **118**, 11278–11282.
- Wang, J., Balazs, Y.S. and Thompson, L.K. (1997) Solid-state REDOR NMR distance measurements at the ligand site of a bacterial chemotaxis membrane receptor. *Biochemistry*, **36**, 1699–1703.
- Long, J.R., Dindot, J.L., Zebroski, H., Kiihne, S., Clark, R.H., Campbell, A.A., Stayton, P.S. and Drobny, G.P. (1998) A peptide that inhibits hydroxyapatite growth is in an extended conformation on the crystal surface. *Proc. Natl Acad. Sci. USA*, **95**, 12083–12087.
- Gullion, T. and Schaefer, J. (1989) Rotational-echo double-resonance NMR. *J. Magn. Reson.*, **81**, 196–200.
- Gullion, T. and Schaefer, J. (1989) Detection of weak heteronuclear dipolar coupling by rotational-echo double-resonance nuclear magnetic resonance. *Adv. Magn. Reson.*, **13**, 57–83.
- Gullion, T. (1997) Measurement of heteronuclear dipolar interactions by rotational-echo, double-resonance nuclear magnetic resonance. *Magn. Reson. Rev.*, **17**, 83–131.
- Dusold, S. and Sebald, A. (2000) Dipolar recoupling under magic angle spinning conditions. In Webb, G. (ed.), *Annual Reports on NMR Spectroscopy*. Academic Press Inc, San Diego, Vol. 41, pp. 185–264.
- Zimmer, C. and Wahnert, U. (1986) Nonintercalating DNA-binding ligands: specificity of the interaction and their use as tools in biophysical, biochemical and biological investigations of the genetic material. *Prog. Biophys. Mol. Biol.*, **47**, 31–112.
- Klevit, R.E., Wemmer, D.E. and Reid, B.R. (1986) ^1H NMR studies on the interaction between distamycin A and a symmetrical DNA dodecamer. *Biochemistry*, **25**, 3296–3303.
- Coll, M., Frederick, C.A., Wang, A.H. and Rich, A. (1987) A bifurcated hydrogen-bonded conformation in the d(a.T) base pairs of the DNA dodecamer d(CGCAAATTTGCG) and its complex with distamycin. *Proc. Natl Acad. Sci. USA*, **84**, 8385–8389.
- Pelton, J.G. and Wemmer, D.E. (1988) Structural modeling of the distamycin a-d(CGCGAATTCGCG) $_2$ complex using 2D NMR and molecular mechanics. *Biochemistry*, **27**, 8088–8096.
- Pelton, J.G. and Wemmer, D.E. (1989) Structural characterization of a 2:1 distamycin a.D(CGCAAATTTGCG) complex by two-dimensional NMR. *Proc. Natl Acad. Sci. USA*, **86**, 5723–5727.
- Pelton, J.G. and Wemmer, D.E. (1990) Structure and dynamics of distamycin A with d(CGCAAATTTGCG):D(GCCAAATTTGCG) at low drug:DNA ratios. *J. Biomol. Struct. Dyn.*, **8**, 81–97.
- Wang, H., Liaw, Y., Robinson, H. and Gao, Y. (1990) Mutual conformational adaptation of both ligand and receptor in anti-tumor drug-DNA complexes. In Pullman, B. and Jortner, J. (eds), *Molecular Basis of Specificity in Nucleic Acid-Drug Interactions*. Kluwer, Dordrecht, The Netherlands, pp. 1–21.
- Boehncke, K., Nonella, M., Schulten, K. and Wang, A.H. (1991) Molecular dynamics investigation of the interaction between DNA and distamycin. *Biochemistry*, **30**, 5465–5475.
- Rentzperis, D., Kupke, D.W. and Marky, L.A. (1992) Differential hydration of homopurine sequences relative to alternating purine/pyrimidine sequences. *Biopolymers*, **32**, 1065–1075.
- Fagan, P. and Wemmer, D.E. (1992) Cooperative binding of distamycin-A to DNA in the 2:1 mode. *J. Am. Chem. Soc.*, **114**, 1080–1081.

21. Stringer, J. and Drobny, G.P. (1998) Methods for the analysis and design of a solid state nuclear magnetic resonance probe. *Rev. Sci. Instrum.*, **69**, 3384–3391.
22. Bak, M., Rasmussen, J.T. and Nielsen, N.C. (2000) Simpson: a general simulation program for solid-state NMR spectroscopy. *J. Magn. Reson.*, **147**, 296–330.
23. Pjura, P.E., Grzeskowiak, K. and Dickerson, R.E. (1987) Binding of Hoechst 33258 to the minor groove of B-DNA. *J. Mol. Biol.*, **197**, 257–271.
24. Tabernero, L., Verdagner, N., Coll, M., Fita, I., Van Der Marel, G.A., Van Boom, J.H., Rich, A. and Aymami, J. (1993) Molecular structure of the A-tract DNA dodecamer d(CGCAAATTTGCG) complexed with the minor groove binding drug netropsin. *Biochemistry*, **32**, 8403–8410.
25. Nunn, C.M. and Neidle, S. (1995) Sequence-dependent drug binding to the minor groove of DNA: crystal structure of the DNA dodecamer d(CGCAAATTTGCG)₂ complexed with propamidine. *J. Med. Chem.*, **38**, 2317–2325.
26. Mitra, S.N., Wahl, M.C. and Sundaralingam, M. (1999) Structure of the side-by-side binding of distamycin to d(GTATATAC)₂. *Acta Crystallogr. D*, **55**, 602–609.
27. Merritt, M., Sigurdsson, S.T. and Drobny, G.P. (1999) Long-range measurements to the phosphodiester backbone of solid nucleic acids using 31P-19F REDOR NMR. *J. Am. Chem. Soc.*, **121**, 6070–6071.
28. Fratini, A.V., Kopka, M.L., Drew, H.R. and Dickerson, R.E. (1982) Reversible bending and helix geometry in a B-DNA dodecamer: CGCGAATTCGCG. *J. Biol. Chem.*, **257**, 14686–14707.
29. Laughton, C. and Luisi, B.F. (1998) The mechanics of minor groove width variation in DNA and its implications for the accommodation of ligands. *J. Mol. Biol.*, **288**, 953–963.
30. Gavathiotis, E., Sharman, G.J. and Searle, M.S. (2000) Sequence-dependent variation in DNA minor groove width dictates orientational preference of Hoechst 33258 in A-tract recognition: solution NMR structure of the 2:1 complex with d(CTTTTGCAAAAG)₂. *Nucleic Acids Res.*, **28**, 728–735.
31. Bostock-Smith, C.E., Harris, S.A., Laughton, C.A. and Searle, M.A. (2001) Induced fit DNA recognition by a minor groove binding analogue of Hoechst 33258: fluctuations in DNA A tract structure investigated by NMR and molecular dynamics simulations. *Nucleic Acids Res.*, **29**, 693–702.
32. Wellenzohn, B., Flader, W., Winger, R.H., Hallbrucker, A., Mayer, E. and Liedl, K.R. (2002) Influence of netropsin's charges on the minor groove width of d(CGCGAATTCGCG)₂. *Biopolymers*, **61**, 276–286.
33. Saenger, W. (1984) *Principles of Nucleic Acid Structure*. Springer-Verlag, New York, NY, pp. 220–241, 253–282.
34. Dickerson, R.E. (1983) Base sequence and helix structure variation in B and A DNA. *J. Mol. Biol.*, **166**, 419–441.
35. Nelson, H.C., Finch, J.T., Luisi, B.F. and Klug, A. (1987) The structure of an oligo(dA).oligo(dT) tract and its biological implications. *Nature*, **330**, 221–226.
36. Kopka, M.L., Yoon, C., Goodsell, D., Pjura, P. and Dickerson, R.E. (1985) The molecular origin of DNA-drug specificity in netropsin and distamycin. *Proc. Natl Acad. Sci. USA*, **82**, 1376–1380.
37. Kim, S.G. and Reid, B.R. (1992) Solution structure of the T_nA_n DNA duplex GCCGTTAACGCG containing the hpaI restriction site. *Biochemistry*, **31**, 12103–12116.
38. Aramini, J.M., Mujeeb, A. and Germann, M.W. (1998) NMR solution structures of [d(CGGAAT-3'-3'-alphaT-5'-5'-CGC)₂] and its unmodified control. *Nucleic Acids Res.*, **26**, 5644–5654.
39. Tjandra, N., Tate, S., Ono, A., Kainosho, M. and Bax, A. (2000) The NMR structure of a DNA dodecamer in an aqueous dilute liquid crystalline phase. *J. Am. Chem. Soc.*, **122**, 6190–6200.
40. Kuszewski, J., Schwieters, C. and Clore, G.M. (2001) Improving the accuracy of NMR structures of DNA by means of a database potential of mean force describing base-base positional interactions. *J. Am. Chem. Soc.*, **123**, 3903–3918.
41. Barbic, A., Zimmer, D.P. and Crothers, D.M. (2003) Structural origins of adenine-tract bending. *Proc. Natl Acad. Sci. USA*, **100**, 2369–2373.
42. Edwards, K.J., Brown, D.G., Spink, N., Skelly, J.V. and Neidle, S. (1992) Molecular structure of the B-DNA dodecamer d(CGCAAATTTGCG)₂. An examination of propeller twist and minor-groove water structure at 2.2 Å resolution. *J. Mol. Biol.*, **226**, 1161–1173.
43. Hud, N.V. and Feigon, J. (1997) Localization of divalent metal ions in the minor groove of DNA A-tracts. *J. Am. Chem. Soc.*, **119**, 5756–5757.
44. Hud, N.V., Sklenar, V. and Feigon, J. (1999) Localization of ammonium ions in the minor groove of DNA duplexes in solution and the origin of DNA A-tract bending. *J. Mol. Biol.*, **286**, 651–660.
45. Hamelberg, D., McFail-Isom, L., Williams, L.D. and Wilson, W.D. (2000) Flexible structure of DNA: ion dependence of minor-groove structure and dynamics. *J. Am. Chem. Soc.*, **122**, 10513–10520.
46. Shui, X., Sines, C.C., McFail-Isom, L., Vanderveer, D. and Williams, L.D. (1998) Structure of the potassium form of CGCAATTCGCG: DNA deformation by electrostatic collapse around inorganic cations. *Biochemistry*, **37**, 16877–16887.
47. Wellenzohn, B., Flader, W., Winger, R.H., Hallbrucker, A., Mayer, E. and Liedl, K.R. (2001) Significance of ligand tails for interaction with the minor groove of B-DNA. *Biophys. J.*, **81**, 1588–1599.